Nature Environment and Pollution Technology
An International Quarterly Scientific Journal
p-ISSN: 0972-6268
(Print copies up to 2016)
e-ISSN: 2395-3454
Vol. 22 No. 2 pp. 741-753 2023
Original Research Paper
https://doi.org/10.46488/NEPT.2023.v22i02.017
Open Access Journal

Measurement of Black Carbon Absorption Coefficients Using an Aethalometer and Their Association with Visibility

Khadeejeh M. Hamasha*†
*Department of Physics, Yarmouk University, Jordan
†Corresponding author: Khadeejeh M. Hamasha; khamasha@yu.edu.jo

Nat. Env. & Poll. Tech.
Website: www.neptjournal.com

Received: 07-11-2022
Revised: 16-12-2022
Accepted: 05-01-2023

Key Words:
Black carbon
Absorption coefficient
Fossil fuel
biomass burning
Visibility

ABSTRACT

Black carbon (BC) is a pollutant aerosol affecting climate and human health. Light absorption coefficients of black carbon (B_{abs}) were measured using an aethalometer model AE33 at wavelengths 370, 470,520,660,880, and 950 nm. B_{abs} for the seven wavelengths at seven sites in Jordan fluctuated with time and peaked at rush hours. The daily average values for all sites were inversely proportional to the wavelength. The average daily visibility values in the seven Jordan sites varied between 72 km and 211km. In the Irbid site, the daily average visibility values for 7-13 Nov. 2021 varied between 43 km and 107 km. BC varied from hour to hour and from day to day. The daily average values of BC in Irbid for the period of 7 -13 Nov. 2021 varied between 2.24 μg.m^{-3} and 4.66 μg.m^{-3}. BC peaked at the rush hour and had the lowest values on Friday. About 90% of the measured BC was from fossil fuel sources and 10% from biomass-burning sources.

INTRODUCTION

Light-absorbing carbon particles are the most abundant and efficient light-absorbing component in the atmosphere in the visible spectrum (Liu et al. 2020, Ziyong et al. 2022). It typically depends inversely on wavelength. Organic carbon is strongly wavelength dependent, with increased absorption for UV and short wavelength visible radiation, but hardly at all at 870 nm. Black carbon is very likely to dominate at 870 nm. Black carbon, the main constituent of soot, is almost exclusively responsible for aerosol light absorption at long-wavelength visible radiation and near-infrared wavelengths. This type of pollution is sometimes referred to as black carbon pollution. Air pollution caused by black carbon particles has been a major problem since the beginning of the industrial revolution and the development of the internal combustion engine. Scientific publications dealt with soot and smoke analysis as early as 1896. Mankind has become so dependent on burning fossil fuels (petroleum products, coal, and natural gas) that all combustion-related emissions now constitute a serious and widespread problem for human health and the entire global environment. The absorption of solar radiation by black carbon is expected to lead to the heating of the atmosphere since the light energy is converted into thermal energy. This heating effect would be expected to be most important in polluted urban areas. Black carbon aerosol light absorption reduces the amount of sunlight available at the surface to drive atmospheric circulation and boundary layer development. Even burning wood and charcoal in fireplaces and barbeques can release significant soot into the air. Some of these pollutants can be created by indoor activities such as smoking and cooking.

An aethalometer usually measures black Carbon concentrations. Aethalometer is an instrument that uses the filter-based technique to measure the aerosol absorption coefficients (Babs) at a specific wavelength (Drinovec et al. 2017, Olson et al. 2015, Wang et al. 2011, Sandradewi 2008). B_{abs} is proportional to the concentration of the black carbon. A new generation of aethalometer, model AE33 (Magee Scientific Corp. 2015), uses the DualSpot technology. In this technology, simultaneous analysis of the absorption of light by the aerosol collected on two parallel points on the filter tape at different loading rates. The two results are combined to eliminate changes in response due to load effects during the measurement (Drinovec et al. 2015).

MATERIALS AND METHODS

In this study, the B_{abs} of black carbon were measured using the aethalometer for seven different wavelengths at different sites in Jordan. Measurement sites were Irbid, Amman, Zarqa, Mafraq, Ajloun, North Shuna, and Tapqat Fahel. Measurement in each site was for one day except in Irbid city, which was for a week. The measurement site in Irbid was chosen to be in Yarmouk University at the location of the Science Building. This building is next to the university's northern gate on the city's most crowded street.

Aethalometer model AE33 (Magee Scientific, USA) was used to measure the absorption coefficients in this study. Aethalometer AE33 is an instrument used to measure the black carbon concentration in real-time by measuring the light absorption on an aerosol-loaded filter. Using dual-spot technology and multi-seven-wavelength optical analysis, the AE33 provides accurate data on a time scale as rapid as 1 minute. An external pump is used to draw the air sample at a flow rate of 5 liters per minute through the inlet port of the aethalometer. The sample that enters the optical chamber is deposited on two spots on the filter tape at different loading rates. The instrument then performs an optical analysis of the sample by measuring the transmission of light emitted by the optical source at seven wavelengths; 370, 470, 520, 590, 660, 880, and 950 nm through the two spots containing the sample compared to the transmission of the unloaded portion of the filter tape, which acts as a reference region. Because the instrument is characterized by cumulative deposition of the sample on the filter, it depends on the change of the light attenuation every minute to calculate the concentration of black carbon.

RESULTS AND DISCUSSION

In this study, aethalometer AE33 was used to measure the light absorption coefficients at seven wavelengths in seven sites in Jordan in 2021. Diurnal measurements were performed at seven sites (Table 1), and a one-week-long measurement at site seven. Black carbon concentrations (BC) were calculated from the absorption coefficients at a wavelength of 880 nm (Sandradewi 2008, Yang et al. 2009). Also, absorption coefficients at pairs of wavelengths assessed the component apportionment of the BC from fossil fuel (BCff) and biomass-burning (BCbb) sources.

Table 1: Site names and dates for AE33 measurements in Jordan in 2021.

Site	Site Name	Date of Measurement
1	Mafraq	9/9/2021
2	North Shuna	13/9/2021
3	Tabqat Fahel	15/9/2021
4	Ajloun	20/9/2021
5	Amman	4/10/2021
6	Zarqa	6/10/2021
7	Irbid	7/11/2021

Table 2 shows the average values of B_{abs} and BC with their sources for the seven wavelengths at the study sites. These measurements were taken by AE33 during the day for one day at each site. B_{abs} is inversely proportional to the wavelength of all sites, as shown in Fig. 1. Irbid (site 7) had the highest values for B_{abs}, while Tabqat fahel (site 3) had the lowest. Irbid is a crowded city in northern Jordan, close to the border with Syria. About 90% of the measured BC was from fossil fuel sources.

Fig. 2 shows B_{abs} for seven wavelengths in Mafraq city on 9 Sep 2021. It's clear from the figure that B_{abs} is inversely proportional to the wavelength. The average values of B_{abs} for the seven wavelengths ranged between 10.6 Mm^{-1} for the

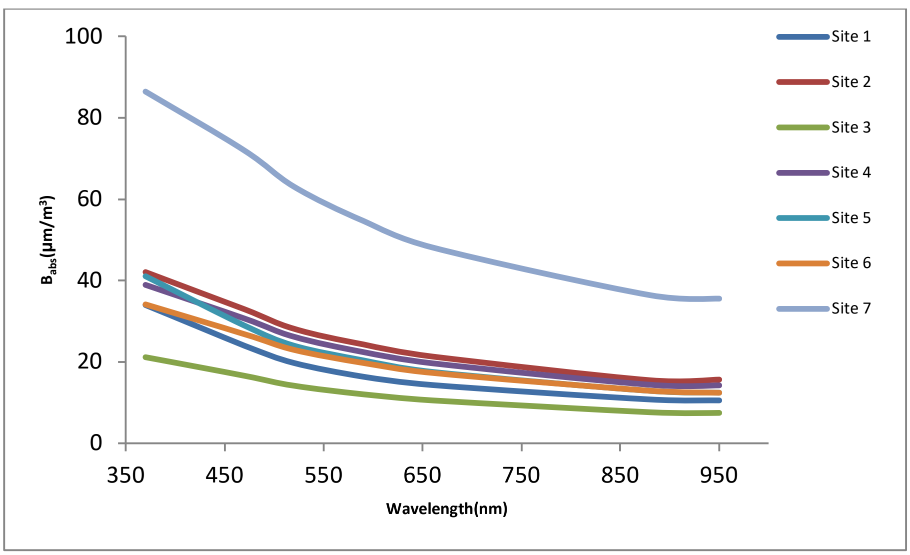

Fig. 1: Average values of light absorption coefficients at seven sites from Jordan for wavelengths 370, 470, 520, 590, 660, 880, and 950 nm.

Table 2: Diurnal average values of the absorption coefficients for the seven sites in Jordan.

Site	$\overline{B}_{abs}(Mm^{-1})$ (370 nm)	$\overline{B}_{abs}(Mm^{-1})$ (470 nm)	$\overline{B}_{abs}(Mm^{-1})$ (520 nm)	$\overline{B}_{abs}(Mm^{-1})$ (590 nm)	$\overline{B}_{abs}(Mm^{-1})$ (660 nm)	$\overline{B}_{abs}(Mm^{-1})$ (880 nm)	$\overline{B}_{abs}(Mm^{-1})$ (950 nm)	BC ($\mu g.m^{-3}$)	BC_{bb} ($\mu g.m^{-3}$)	BC_{ff} ($\mu g.m^{-3}$)
1	33.99 ± 8.90	24.02 ± 6.09	19.77 ± 5.06	16.37 ± 4.07	14.30 ± 3.39	10.74 ± 2.62	10.56 ± 2.44	1.382 ± 0.337	0.172 ± 0.075	1.210 ± 0.262
2	42.06 ± 5.43	32.94 ± 3.85	28.13 ± 3.19	24.29 ± 2.38	21.34 ± 2.18	15.48 ± 1.35	15.64 ± 1.08	1.773 ± 1.298	0.102 ± 0.534	1.671 ± 1.196
3	21.17 ± 3.38	16.58 ± 2.69	14.13 ± 2.48	12.06 ± 2.13	10.53 ± 1.79	7.62 ± 1.20	7.44 ± 1.06	0.981 ± 0.483	0.104 ± 0.163	0.876 ± 0.442
4	38.95 ± 9.81	30.69 ± 7.34	26.18 ± 6.21	22.43 ± 5.52	19.68 ± 4.60	14.35 ± 3.72	14.24 ± 3.49	1.846 ± 1.810	0.142 ± 0.132	1.704 ± 1.811
5	41.07 ± 5.09	28.95 ± 2.90	24.01 ± 2.38	20.35 ± 2.31	17.54 ± 1.79	12.86 ± 1.33	12.45 ± 1.31	1.654 ± 0.171	0.245 ± 0.014	1.409 ± 0.156
6	34.09 ± 21.51	26.85 ± 8.41	22.96 ± 5.63	19.77 ± 4.55	17.27 ± 3.54	12.92 ± 2.04	12.46 ± 2.21	1.663 ± 0.499	0.115 ± 0.160	1.547 ± 0.459
7	86.47 ± 42.17	71.96 ± 35.88	63.07 ± 31.30	54.64 ± 26.70	48.13 ± 2.64	36.38 ± 17.03	33.54 ± 15.20	5.152 ± 3.197	0.446 ± 0.502	4.706 ± 3.083

wavelength of 950 nm and 33.9 Mm^{-1} for the wavelength of 370 nm. For all wavelengths, B_{abs} values fluctuate with two peaks, one at 11:31 am and the other at 12:30 pm. Using the B_{abs} data for pairs of wavelengths, it was found that 12% of the BC was from biomass-burning sources and 88% from the fossil fuel source.

Fig. 3 shows B_{abs} for seven wavelengths in North Shuna city on 13 September 2021. It's clear from the figure that B_{abs} is inversely proportional to the wavelength. The average values of B_{abs} for the seven wavelengths ranged between 15.6Mm^{-1} for the wavelength of 950 nm and 42.1 Mm^{-1} for the wavelength of 370 nm. For all wavelengths, B_{abs} values fluctuate with time. Using the B_{abs} data for pairs of wavelengths, it was found that 6% of the BC was from biomass-burning sources and 94% from the fossil fuel source.

Fig. 4 shows B_{abs} for seven wavelengths in Tabqat Fahel city on 15 September 2021. It's clear from the figure that B_{abs} is inversely proportional to the wavelength. The average values of B_{abs} for the seven wavelengths ranged between 7.4 Mm^{-1} for the wavelength of 950 nm and 21.2 Mm^{-1} for the wavelength of 370 nm. For all wavelengths, B_{abs} values fluctuate with time. Using the B_{abs} data for pairs of wavelengths, it was found that 11% of the BC was from biomass-burning sources and 89% from the fossil fuel source.

Fig. 5 shows B_{abs} for seven wavelengths in Ajloun city on 20 September 2021. It's clear from the figure that B_{abs} is inversely proportional to the wavelength. The average values of B_{abs} for the seven wavelengths ranged between 14.2 Mm^{-1} for the wavelength of 950 nm and 38.9 Mm^{-1} for the wavelength of 370 nm. For all wavelengths, B_{abs} values fluctuate with time. Using the B_{abs} data for pairs of wavelengths, it was found that 8% of the BC was from biomass burning and 92% from fossil fuel sources.

Fig. 6 shows B_{abs} for seven wavelengths in Amman city on 4 October 2021. It's clear from the figure that B_{abs} is inversely proportional to the wavelength. The average values of B_{abs} for the seven wavelengths ranged between 12.5 Mm^{-1} for the wavelength of 950 nm and 41.1 Mm^{-1} for the wavelength of 370 nm. For all wavelengths, B_{abs} values fluctuate with time. Using the B_{abs} data for pairs of wavelengths, it was found that 15% of the BC was from biomass-burning sources and 85% from the fossil fuel source.

Fig. 7 shows B_{abs} for seven wavelengths in Zarqa city on 6 October 2021. It's clear from the figure that B_{abs} is inversely proportional to the wavelength. The average values of B_{abs} for the seven wavelengths ranged between 12.5 Mm^{-1} for the wavelength of 950 nm and 34.1 Mm^{-1}

for the wavelength of 370 nm. For all wavelengths, B_{abs} values fluctuate with time. Using the B_{abs} data for pairs of wavelengths, it was found that 7% of the BC was from biomass-burning sources and 93% from the fossil fuel source.

Fig. 8 shows B_{abs} for seven wavelengths in Irbid city on 7 November 2021. It's clear from the figure that B_{abs} is inversely proportional to the wavelength. The average values of B_{abs} for the seven wavelengths ranged between

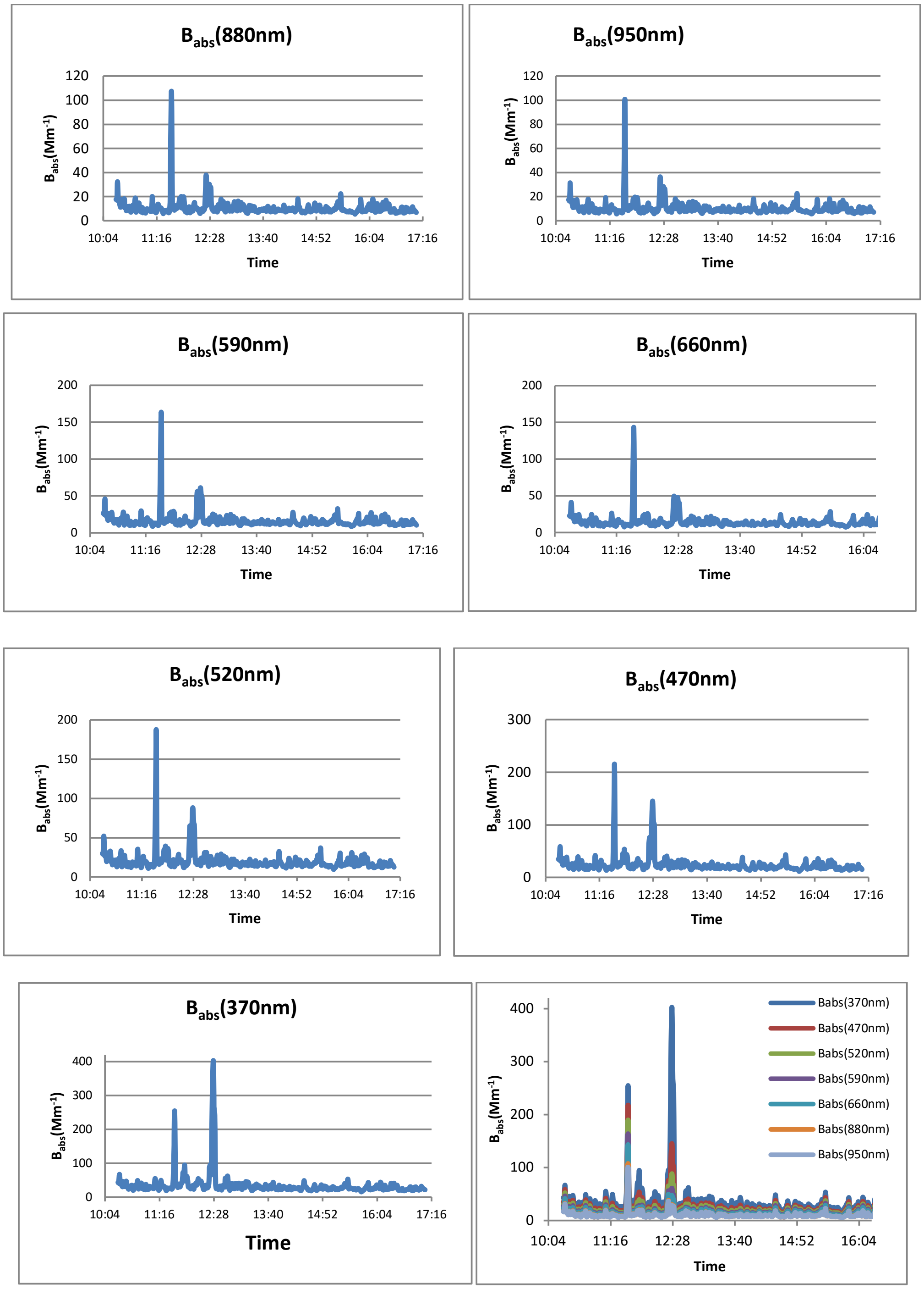

Fig. 2: Diurnal time series of B_{abs} in Mafraq city on 9 September 2021 for the wavelengths 370, 470, 520, 590, 660, 880, and 950nm.

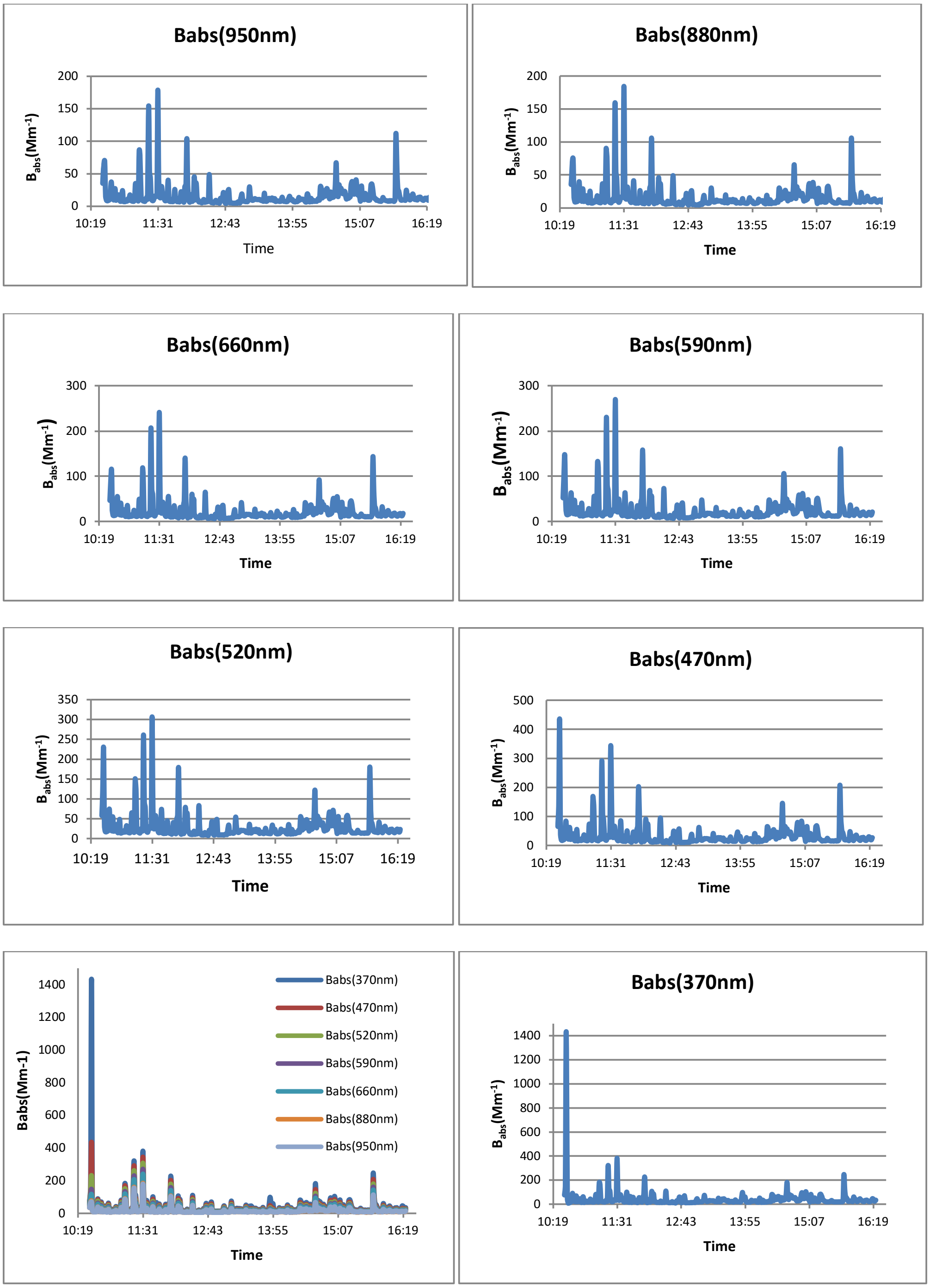

Fig. 3: Diurnal time series of B_{abs} in North Shuna city on 13 September 2021 for the wavelengths 370, 470, 520, 590, 660, 880, and 950nm.

33.5 Mm^{-1} for the wavelength of 950 nm and 86.5 Mm^{-1} for the wavelength of 370 nm. For all wavelengths, B_{abs} values fluctuate with time. Using the B_{abs} data for pairs of wavelengths, it was found that 9% of the BC was from biomass-burning sources and 91% from the fossil fuel source.

Visibility can be calculated from the absorption coefficients at the wavelength of 520nm using the Koschmieder equation (Middleton 1952); $Vis = \frac{3.912}{B_{ATN}}$, where B_{ATN} is the attenuation coefficient of the light due to

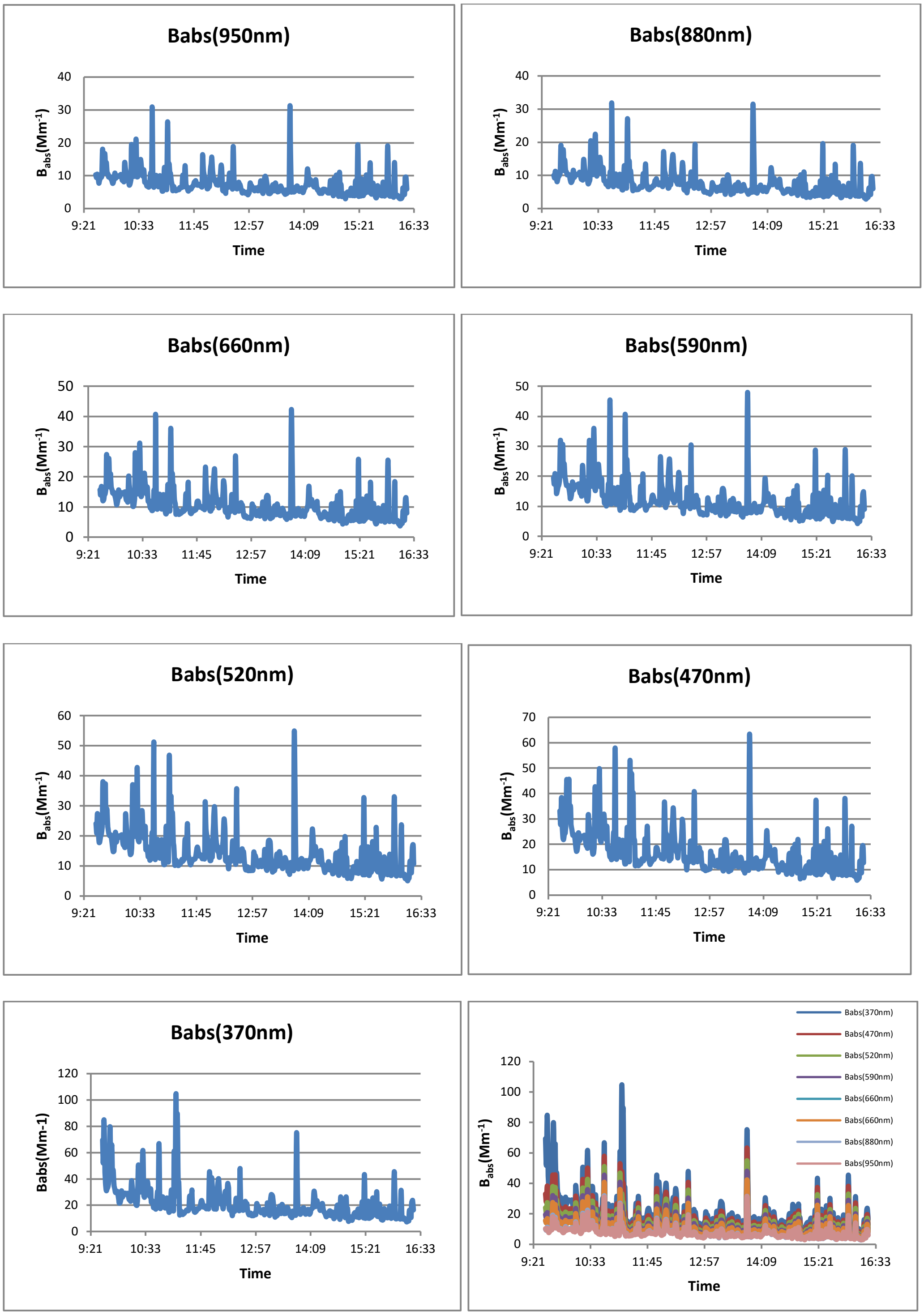

Fig. 4: Diurnal time series of B_{abs} in Tabqat Fahel city on 15 September 2021 for the wavelengths 370, 470, 520, 590, 660, 880, and 950nm.

scattering and atmospheric absorption by particles and gases. For the AE33 instrument, B_{ATN} can be calculated from B_{abs} by $B_{ATN} = 1.57\ B_{abs}$.

Fig. 9 shows the visibility variation during the daytime of the seven sites in Jordan. As seen from the figure, Visibility varies with time and depends on the amount of pollutant

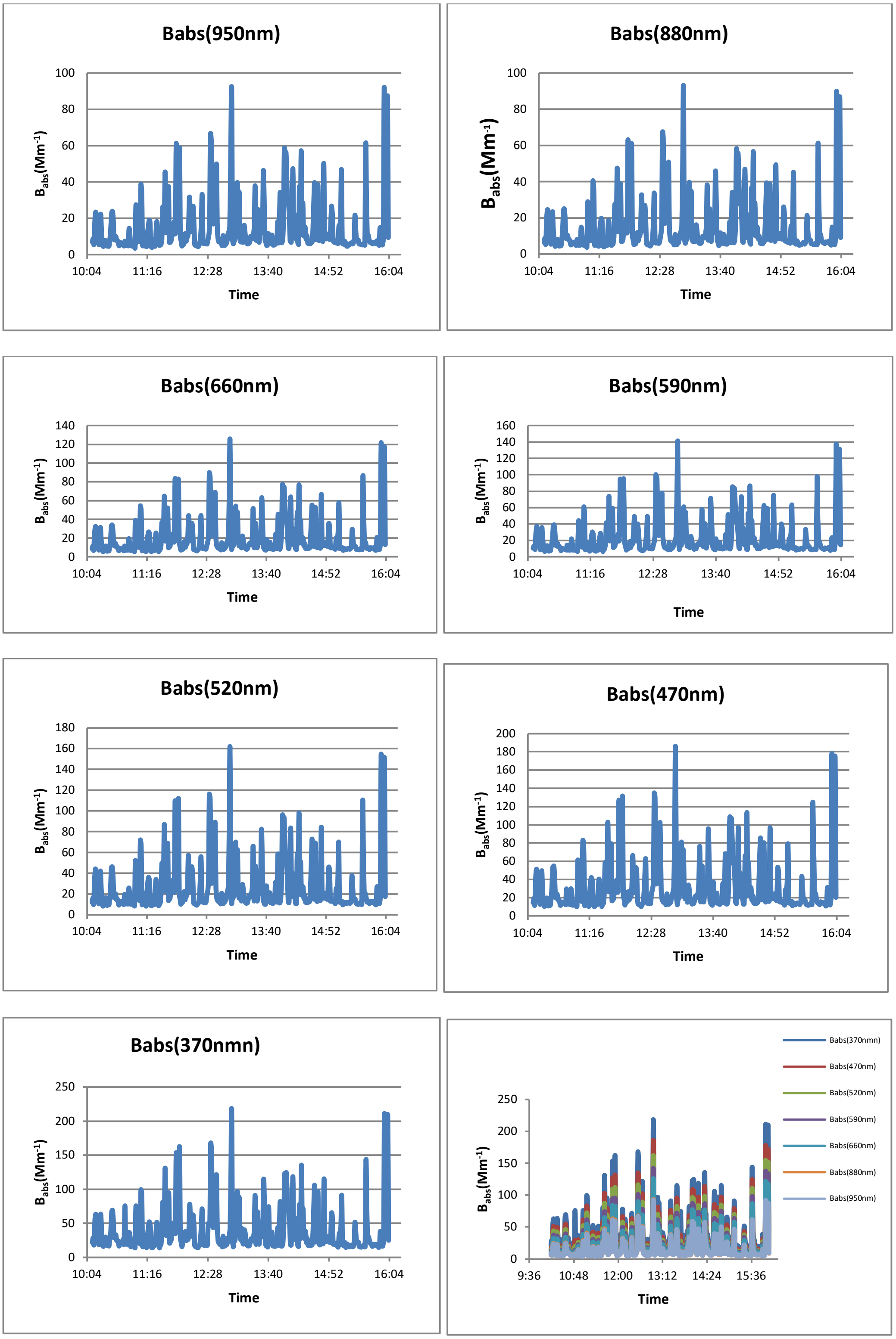

Fig. 5: Diurnal time series of B_{abs} in Ajloun city on 20 September 2021 for the wavelengths 370, 470, 520, 590, 660, 880, and 950nm.

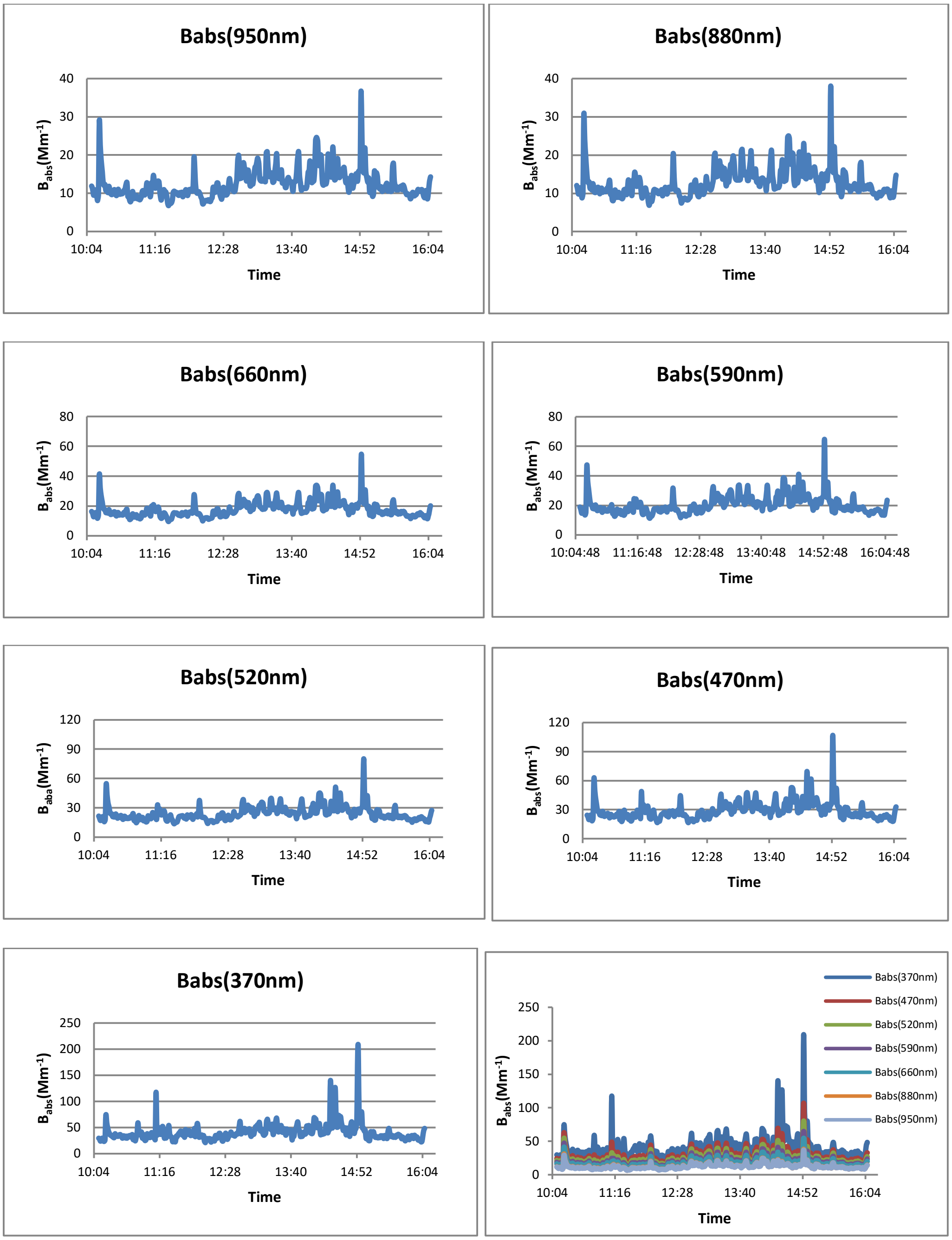

Fig. 6: Diurnal time series of B_{abs} in Amman city on 4 October 2021 for the wavelengths 370, 470, 520, 590, 660, 880, and 950nm.

particles that scatter or absorb lights on the sight path. Visibility decreases with increasing pollutants. The daily average visibility values varied between 72 km at Irbid city and 211 km at Tabqat Fahel. The daily average visibility values showed that the most polluted site by aerosols from the study areas was Irbid, followed by Zarqa, then Amman. Even for one area, the average visibility changes from day to day according to the clearness of the sky from pollutants. Fig. 10 shows a chart of the daily visibility variation for the Irbid site during 7-13 October 2021.

As site seven had the lowest visibility, we studied the black carbon concentration for this site for one week. Fig. 11 shows the variation of BC in Irbid city during the period (7-13) Nov 2021. BC concentrations fluctuated between 0

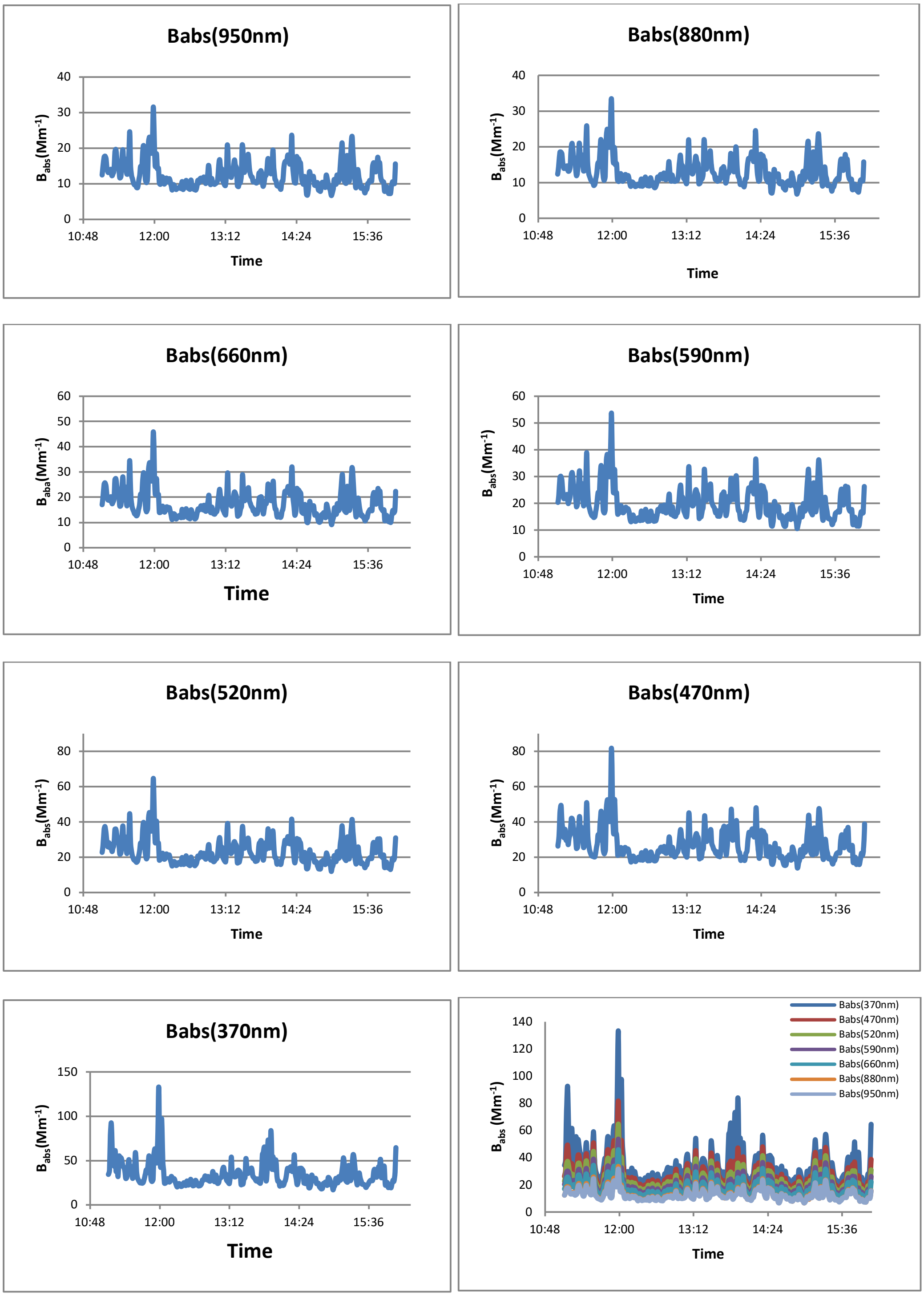

Fig. 7: Diurnal time series of B_{abs} in Zarqa city on 6 October 2021 for the wavelengths 370, 470, 520, 590, 660, 880, and 950nm.

and 10,000 ng.m^{-3} and peaked around rush hours. Irbid is a city that is very crowded with means of transportation. Irbid has a population of about one million people and has many restaurants, cafes, and factories scattered around it, besides Yarmouk University, which has 40,000 students. Also, Irbid is close to the Syrian and Palestinian

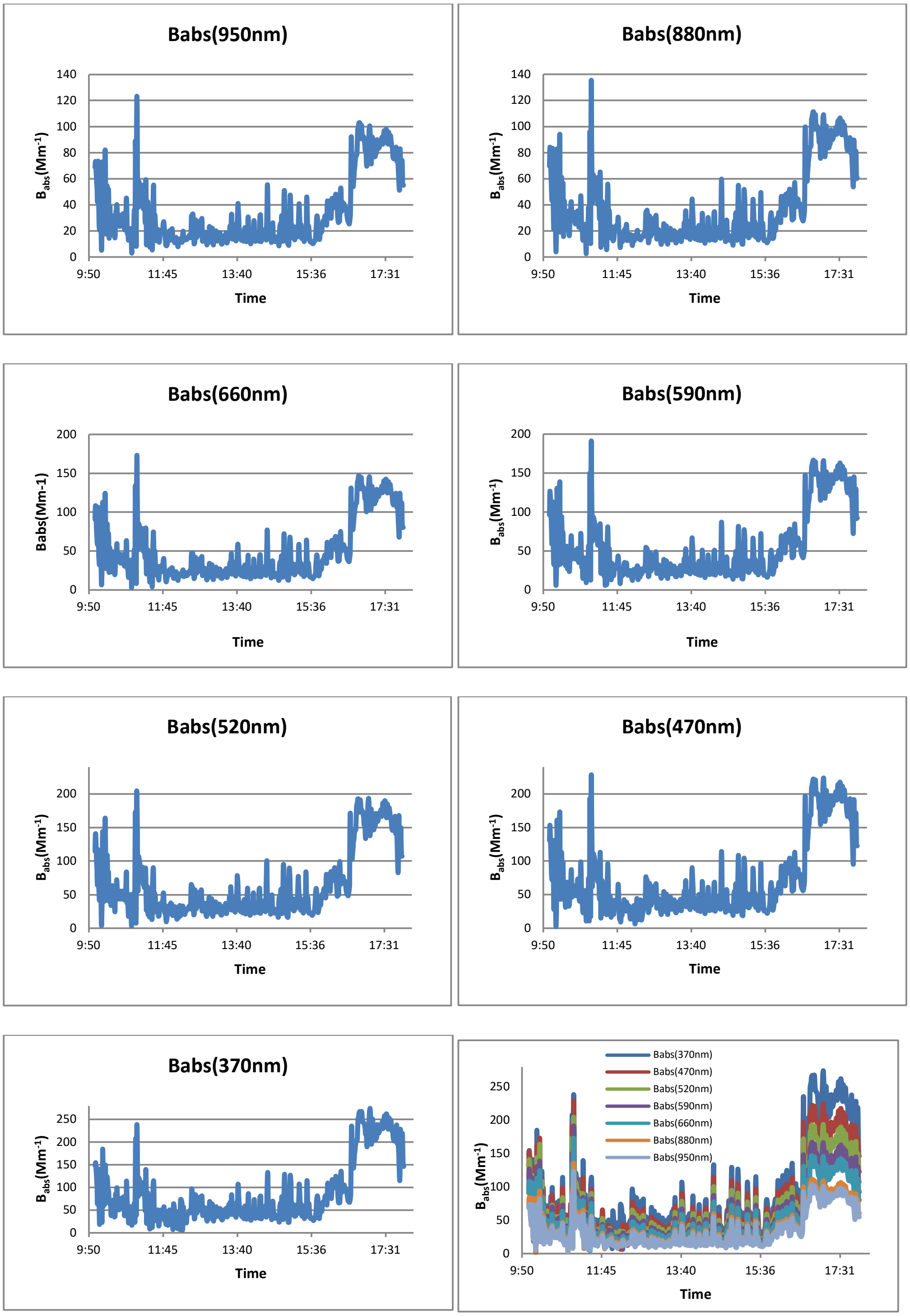

Fig. 8: Diurnal time series of B_{abs} in Irbid city on 7 November 2021 for the wavelengths 370, 470, 520, 590, 660, 880, and 950nm.

borders, increasing the black carbon pollution sources. The daily average values of BC were different from day to day, and Friday had the lowest value of BC, as seen in Fig. 12.

CONCLUSION

B_{abs} in Jordan fluctuated with time and peaked at rush hours. The daily average values of B_{abs} are inversely proportional to the wavelengths. The daily average visibility values are inversely proportional to the values of BC. BC varied from hour to hour and from day to day. BC peaked during the rush hours and had the lowest values on Friday. Most of the measured BC in Jordan is from fossil fuel sources. The Irbid city has the highest values of aerosols in Jordan.

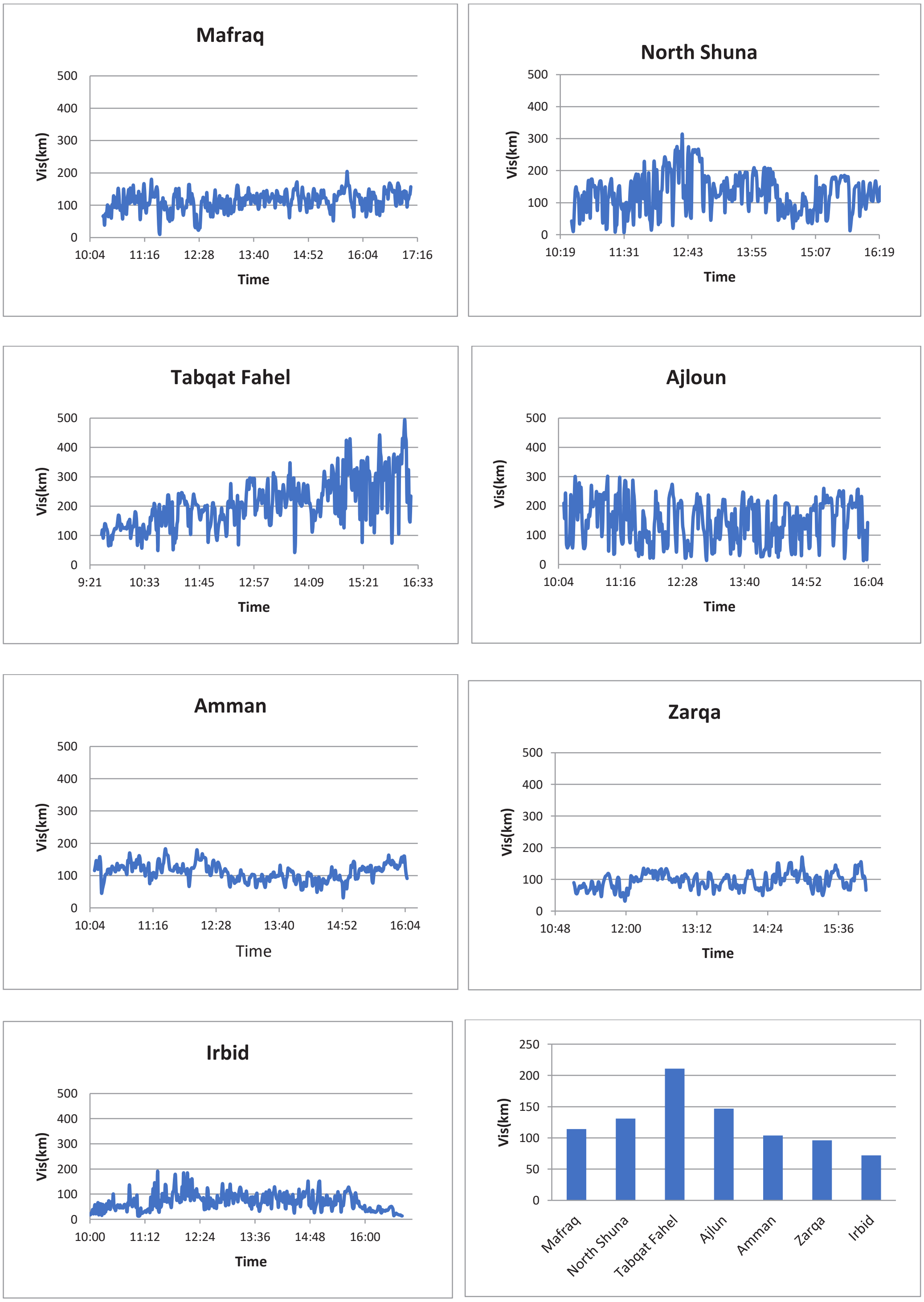

Fig. 9: Diurnal visibility variation in the seven sites in Jordan.

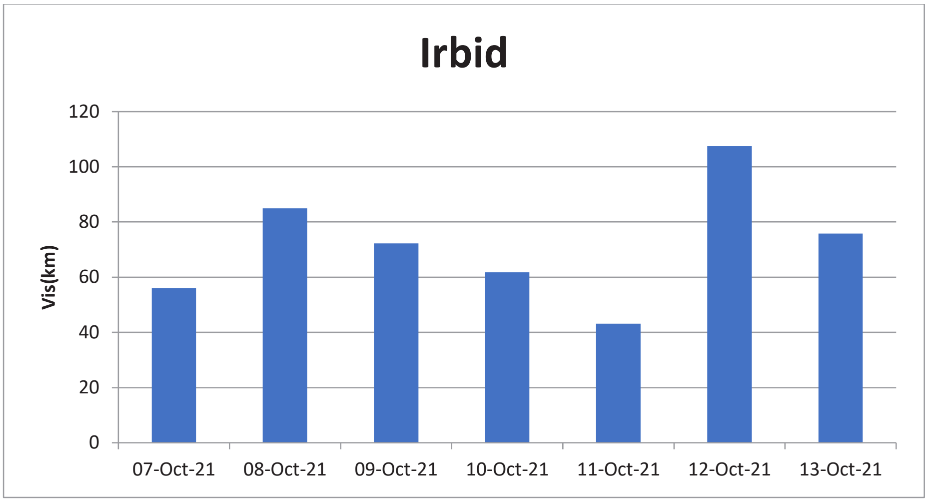

Fig. 10: Dailly average visibility values in site 7 during 7-13 October 2021.

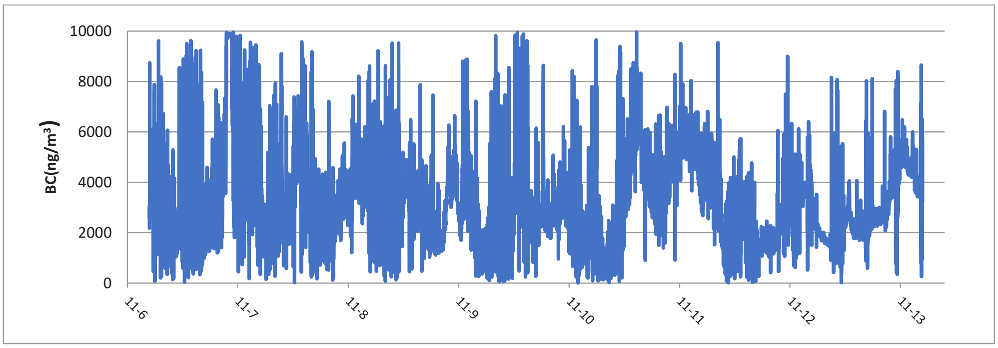

Fig. 11: Time series of BC in Irbid city during the period of 7-13 November 2021.

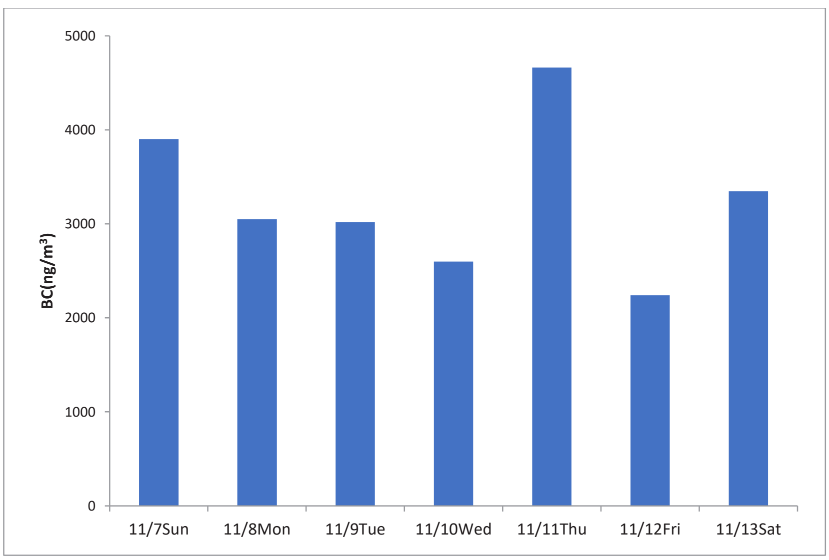

Fig. 12: The daily average value of BC concentrations during the period of 7-13 November 2021 in Irbid city.

ACKNOWLEDGMENT

We thank Scientific Research and Graduate Studies Deanship at Yarmouk University for supporting this work with Grant No. 18/2019.

REFERENCES

Drinovec, L., Močnik, G., Zotter, P., Prévôt, A., Ruckstuhl, C., Coz, E., Rupakheti, M., Sciare, J., Müller, T. and Wiedensohler, A. 2015. The dual-spot aethalometer: an improved measurement of aerosol black carbon with real-time loading compensation. Atmos. Meas. Tech., 8: 1965-1979. https://doi.org/10.5194/ amt-8-1965-2015.

Drinovec, L., Gregoric, A., Zotter P., Wolf R., Bruns E.A., Prevot A., Jean-Eudes Petit J., Favez O., Sciare J., Arnold I., Chakrabarty R., Moosmüller H., Filep A. and Mocnik, G. 2017. The filter-loading effect by ambient aerosols in filter absorption photometers depends on the coating of the sampled particles. Atmos. Meas. Tech., 10: 1043-1059. https://doi.org.10.5194/amt-10-1043-2017.

Liu, D., He, C. and Schwarz, J.P. 2020. Lifecycle of light-absorbing carbonaceous aerosols in the atmosphere. Clim. Atmos. Sci., 3: 40. https://doi.org/10.1038/s41612-020-00145-8.

Middleton, W.E.K. 1952. Vision through the Atmosphere. The University of Toronto Press, Toronto.

Olson, M.R., VictoriaGarcia, M., Robinson, M.A., Van Rooy, P., Dietenberger, M.A., Bergin, M. and Schauer, J.J. 2015, Investigation of black and brown carbon multiple-wavelength-dependent light absorption from biomass and fossil fuel combustion source emissions. J. Geophys. Res. Atmos., 120: 6682-6697. https://doi.org/10.1002/2014JD022970.

Sandradewi, J. 2008. Using aerosol light absorption measurements for the quantitative determination of wood burning and traffic emission contributions to particulate.`

Wang, Y., Hopke, P.K., Rattigan, O.V., Xia, X., Chalupa D.C. and Mark J. 2011. Characterization of residential wood combustion particles using the two-wavelength aethalometer. Environ. Sci. Technol., 45: 7387-7393.

Yang, M., Howell, S.G., Zhuang, J. and Huebert, B.J. 2009, Attribution of aerosol light absorption to black carbon, brown carbon, and dust in China – interpretations of atmospheric measurements during EAST AIRE. Atmos. Chem. Phys., 9: 2035–2050. https://doi.org/10.5194/acp-9-2035-2009.

Ziyong, G., Yuxiang, Y., Xiaodong, H., Xiaocong, P., Yuzhen, F., Wei Sun, G., Zhang, D.C., Xinhui, B., Xinming, W. and Ping, P. 2022. The optical properties and in-situ observational evidence for the formation of brown carbon in clouds. Atmos. Chem. Phys., 22(7): 4827-4839.